

Synthesis, Characterization and Photocatalytic Application of the Grassy-Free Standing Titanium dioxide Nanotubes (Gfs –TiNts)

Muniba Yaseen Naz,^{1, a)} Tayyaba Ghani,² Suleman Ahmad,¹ Uroosa Hadi,³ Robab Mehmood,¹ Atta Ullah Shah,³ and Mazhar Mehmood²

¹⁾Department of Physics and Applied Mathematics, Islamabad, Pakistan. Pakistan Institute of Engineering and Applied Sciences (PIEAS), Islamabad

²⁾Department of Metallurgy and Materials Engineering, Pakistan Institute of Engineering and Applied Sciences (PIEAS), Islamabad

³⁾National Institute of Lasers and Optronics, Pakistan Institute of Engineering and Applied Sciences (PIEAS), Islamabad

ABSTRACT: This study aims to synthesize and characterize the Grassy-Free standing TiO₂ nanotubes (G_{fs}-TiNts) and evaluate their performance for the photocatalytic degradation of Electrochromic Black T-dye (EBT). The scalable 2-step anodization technique is selected to formulate the G_{fs}-TiNts. The synthesis route provided ordered and a few micrometers long TiO₂ nanotubes with nanotubular morphology. Initially, Ti base layer is utilized as a substrate for the synthesis of 1-step anodized TiNts. Certain parameters are carefully chosen to synthesize the nanotubes. After 2nd step anodization, the nanotubes are removed from the substrate and obtained as free standing Grassy TiO₂ nanotubes. Furthermore, the various characterizations are also performed including Field-emission Scanning Electron microscopy (FE-SEM), UV-visible spectroscopy (UV-vis), and photoluminescence spectroscopy (PL) respectively. These characterizations confirmed the formation of ordered free standing TiNts. Through these viable characterizations, some morphological, structural and optical properties are also analyzed. The optical band gap for G_{fs}-TiNts is also calculated through tauc-plot method that aided in the requirement for the Photodegradation. At the end, the synthesized nanomaterials were utilized for the photocatalytic conversion of the Electrochromic Black T-dye (EBT). The synthesized TiNts due to their grassy nanotubular morphology and a lower charge recombination resulted in 40% photocatalytic conversion (10mg/L) within 80 minutes Ux-light exposure. Thus, the synthesized G_{fs}-TiNts based nanomaterials can contribute to sustainable environment management through the degradation of various toxic organic dyes.

Received: 22 November 2024

Accepted: 31 December 2024

DOI: <https://doi.org/10.71107/s4bpbn64>

I. INTRODUCTION

In the recent few decades, industries have discharged significant amount of organic pollutants into the environment and posing a serious alarm to environmental species¹. In the light of serious environmental issues,

industrial water waste treatment is becoming more significant in the field of environmental technology². Historically, traditional methods for removing organic pollutants from waste waters included adsorption, biological treatment, coagulation, ultrafiltration, and ion exchange methods¹. These procedures are not effective and may not break down contaminants in waste water. For instance, adsorption technology does not degrade the pollutants, but rather transfer pollutants from one medium to another hence contribute to secondary pollution. Among these various methods the photocatalytic processes have the potential to degrade an extensive range of organic pollutants at ambient conditions without generating harmful intermediates. In this process, photocatalyst can use solar energy to convert it into chemical energy and thus reduces the pollutants. The entire photocatalytic process is usually based on following main steps; charge carriers' generation, sep-

^{a)}Electronic mail: muniba_21@pieas.edu.pk

aration, and consumption by redox reaction. On the photocatalyst surface, the reactive oxygen species and holes can recombine with the donor species leading to degradation of the organic pollutants including dyes³. Photodegradation is a cost-effective method for converting organic contaminants into non-toxic, low-molecular-weight molecules by photo-assisted redox processes⁴.

Currently various semiconductors are used in photocatalysis. The semiconductor photocatalysts, including CdS, SnO₂, WO₃, TiO₂, ZrTiO₄, and ZnO, titania (TiO₂), offer advantages such as transparency, broad band gap, and biological and chemical inertness⁵. Over the last decade, numerous research efforts have been carried out to synthesize various TiO₂ nanostructures for example, nanofibers, nanoparticles, nanotubes etc. The TiO₂ nanoparticles are most widely industrially produced nanostructures. However, compared to other TiO₂ nanostructures the hollow structure in TiO₂ nanotubes results in an enormous accessible surface area. As well as, the morphology and surface area in TiNts is simply controllable^{6,7}. Anodized titanium oxide nanotubes have been used in photocatalysis⁸. TiNts are ideal for this application due to their porous structure, large effective surface area, and good electrochemical and corrosion properties. Controlling the voltage, electrolyte composition, pH, anodization time, and temperature allows for finetuning of nanotube arrays to desired dimensions⁹⁻¹¹. TiNts are commonly manufactured on titanium substrates via anodization, resulting in a vertically aligned and highly ordered nanotube array^{12,13}. This alignment results in a uni-directional charge transport and enhanced charge separation, as well as directional diffusion pathways¹⁴. The TiNts due to being connected to the Ti substrate, requires no further immobilization for application purpose.

Among various organic dyes EBT, an azo dye used in the textile industry which is toxic and carcinogenic due to its chemical stability. Its presence in drinking water can be deadly to human health¹⁵. EBT is an anionic dye with a stable chemical structure that can resist degradation by microbes and light¹⁶. Several photocatalysts have been reported to degrade EBT dye including Eu-doped ZnO, CoCr₂O₄, NiS-Analcime composite, Fe³⁺ and Pt⁴⁺ impregnated TiO₂, among others^{14,17-19}. TiNts for the degradation of various dyes has already been reported in literature. For example, the open-top-tube TiNts was found to be promising in the degradation of methylene blue (MB) reaching 85% photodegradation after 480 min irradiation²⁰. In another study, annealed grassy TiO₂ nanotubes exhibited good photoreduction of Cr(VI) by 100% reduction within 30 min of UV irradiation²¹. In a recent study

by R. Ashaga Sherly et al, the pristine TiNts resulted in 42% photodegradation of methyl violet dye in 500 minutes²². Till now, the research area for the grassy TiNts is yet not widely explored in photo assisted applications.

In this study, pioneering work for the synthesis and characterization of the amorphous Grassy free standing titanium dioxide nanotubes is aimed to explore their potential for dye degradation. The 2-step anodization approach with specified parameters is applied to synthesize the free standing highly ordered nanotubular structures. The morphological, structural and optical properties are determined for the synthesized G_{fs}-TiNts. Specifically, the excellent optical properties and unique grassy nanotubular morphology will enable them to harness light effectively. To the best of our knowledge, till now the grassy TiNts are not widely evaluated for the photodegradation performance of organic dyes and pollutants. Current research is the first attempt to synthesize the anodized G_{fs}-TiNts to degrade the toxic azo dye EBT (10mg/L) in an aqueous solution. This study reveals that instead of being grassy, the presence of an anatase phase and enhanced light absorption properties can result in better photo degradation.

II. METHODOLOGY

The material used as substrate in the present study was titanium (99.6% purity) sheet obtained from online Ti shop (available at <http://www.ti.shop.com>). Chemicals used were ethanol, acetone, deionized water, ethylene glycol, and ammonium fluoride (Sigma Aldrich) for the washing of Ti sheet and making electrolyte, respectively. All the chemicals were of analytical grade and used without any further purification.

Titanium sheets were cut into 2 cm × 4 cm pieces and polished with emery paper to obtain the oxide free, shiny and smooth surface. The sheets were placed in ultrasonic bath and cleaned in acetone, ethanol, and deionized water for 10 minutes each to eliminate surface scums. For the first step anodization, the foils were anodized in an electrolyte solution consisting of ethylene glycol, 0.3wt% NaNH₄F, and 2vol% deionized water. The explanation for using the ethylene glycol electrolyte is explained elsewhere²³. A titanium sheet served as the anode, and the platinum sheet act as the anode. Both anodization steps were carried out at 50 V and 20°C temperature. The first step anodization was carried out for 2 hours. After anodization, the TiO₂ anodized layer was removed by sonication in deionized water for 10 minutes and then dried in air (Table I). This step left a patterned titanium surface

suitable for further anodization. The titanium sheets were subjected to the same anodization conditions as in step-2 for another 4 hours. This process resulted in the formation of a highly ordered TiO₂ nanotube array with improved tubular quality. The anodized samples were soaked in deionized water at room temperature for 5–6 hours. This step detached the TiO₂ nanotube films from the titanium substrate. Thus the self-detached TiNts were collected and ground to get fine powder. The Photo-catalysis performance of Grassy-Free standing TiO₂ nanotubes (Gfs-TiNts) was studied by decolorization of ETB dye. Firstly 20 PPM (10mg/L) solution of ETB dye (PH = 7) was prepared and 6 mg of catalyst was added. After stirring the solution was exposed to a Xenon Lamp light source (254 nm, 150 W) placed at the distance of 15 inches. After every 10 minutes 4 – 5ml solution was extracted and dye concentration was determined by finding absorbance using uv-visible spectrophotometer. The schematics preparation of TiNts is listed below in Figs. 1 and 2.

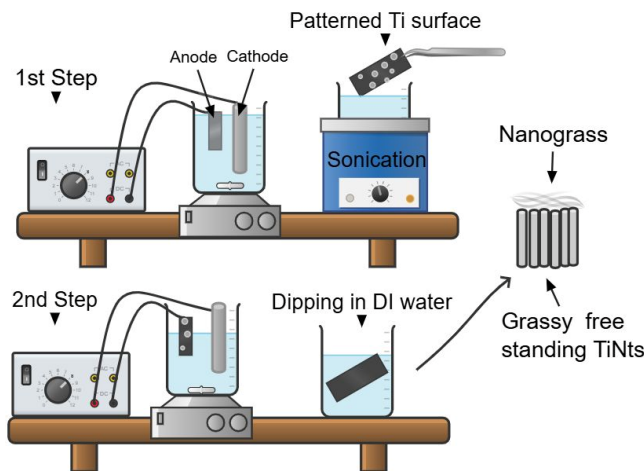


FIG. 1: Schematics for the preparation of Gfs-TiNts.

III. MATERIAL CHARACTERIZATION

The surface morphology, average particle size, crystalline nature, UV-visible absorption peaks and photodegradation were measured. The surface morphology and average particle size was estimated by TESCAN MAIA3 Triglav™ Scanning Electron Microscopy (SEM). The optical properties were studied by Spectro UV-VIS Double Beam UVD3500 Labomed Inc. The photodegradation was conducted under light of a 150 W fluorescent high-pressure Xenon lamp (Philip ML 150 W).



FIG. 2: The grassy free standing TiNts during detachment from Ti Substrate.

IV. RESULTS AND DISCUSSION

A. Morphological analysis

The unique two-step anodization methods are used to create TiNts as seen in the schematic Fig. 3. Fig. 3(a, b) displays the morphology of the free-standing nanotubular grassy nanostructures. Amorphous layers are visible in the SEM image. The free-standing tubular uniformly thick structures are formed with measuring 30 – 35 nm outer diameter. Figures display the top and cross-sectional FE-SEM images. The tube walls which have an inner diameter of roughly 60 – 100 nm well divided into discrete entities. It is evident from the tube top surface has irregular shaped structures as show in Fig. 3 and they have a disintegrated shaped grass that is partially etched with the original tube layer following anodization in the electrolyte based on NH₄ F+ ethylene glycol²⁴. During the anodization mechanism, the first stage anodization in fluoride ions containing electrolyte forms nanotubular layers on the Ti substrate.

With extremely high adhesion, these anodic TiNts arrays are formed perpendicular to the titanium substrate. The tube walls are usually deformed by chemical etching, resulting in the creation of extremely porous TiO₂ nanggrass formations on the tube tops²⁵. The anodized TiO₂ nanggrassy layers must be resilient in the chemical etchant in order to separate from the substrate. In fact, the amorphous oxides are significantly dissolved out in the etchant even if the layer thickness is higher. This procedure results in free-standing TiO₂ nanggrassy

TABLE I: Processing Parameters for Two-Step Treatment

Parameters	First Step	Second Step
Time	2 hours	4 hours
Temperature	20°C	20°C
Voltage	50 V	50 V
Electrolyte	Ethylene Glycol based	Ethylene Glycol based
Treatment	Sonicated in DI water (10 minutes)	Dipped in DI water (5-6 hours)

tubular nanostructures that are used as a photocatalyst to break down dyes.

B. Raman Spectroscopy

Raman spectrum depicts the weak and broad peaks which are linked to the amorphous state's lack of crystallinity as showed in Fig. 4. A prominent peak at around 154 cm^{-1} in the Raman spectra indicates the E1 g vibration mode which is linked to the anatase structure's symmetric stretching vibration of O-Ti-O⁴⁰. The B1 g, A1 g, and Eg modes of the anatase phase were identified as the cause of the vibrations detected at $390.0, 511.4, \text{ and } 632.1 \text{ cm}^{-1}$, respectively. The six Raman-active vibrational modes of anatase-phase TiO₂ are A1 g + 2 B1 g + 3 Eg, per earlier studies²⁶. Symmetric stretching vibration of O-Ti-O, symmetric bending vibration of OTi-O, and anti-symmetric bending vibration of O-Ti-O lead to Eg, B1 g, and A 1 g respectively²⁷. In comparison to the O-Ti-O stretching mode, the Eg peak is more susceptible to oxygen vacancies²⁸. Thus it has confirmed the presence of TiNTs with grassy morphology with a peak for anatase phase TiNTs. Interestingly the tubes are still not annealed but the dipping in deionized water for a long time 5-6 hours can result in spontaneous water assisted reaction. This mild crystallization mechanism involves the dissolution and precipitation processes in which a spatial atomistic order is induced by water molecules²⁹. The effectiveness of the anatase phase in the photocatalysis may be explained by the presence of surface states that trap charge carriers and increase their involvement in the redox reactions. Effective reactant adsorption and interaction with photogenerated species may become possible by the anatase phase's high density of active sites and advantageous surface energy. The anatase phase is known to particularly work well in the UV-induced photocatalysis applications. Thus, the anatase structure in the present investigation may enable an improved production of reactive oxygen species (ROS), which are essential for photocatalytic degradation. Anatase TiNTs are preferred for photocatalytic application as they exhibit a longer carrier charge lifetime as well as being more photoreactive This demon-

strates how important anatase TiNTs are for facilitating the efficient dynamics of electron-hole pairs and surface contacts required for EBT dye degradation^{21,30}.

C. Optical Properties

Fig. 5 shows the optical absorption spectra of amorphous Gfs- TiNTs with Nanggrass layers in wavelength range 200-800 nm. Absorption occurs in the ultraviolet to visible area, with absorption peak at 335 nm, corresponding to the $\pi - \pi^*$ transition³¹. The Fig. 6 illustrates the optical band gap of TiO₂NTs with Nanggrass layer by plotting $(ah\nu)$ vs photon energy ($h\nu$) and extrapolating the straight line to zero absorption to obtain the effective band gap energy (E_g) value. The direct band gap is calculated by using the Stern equation³¹.

$$(ah\nu)^2 = B(h\nu - E_g)$$

The equation includes absorbance (a), light constant (v) in wavelength units, Planck's constant (h), band gap energy (E_g), and a constant (k). To measure the direct band-gap, n is set to 2. The Tauc plots of the absorption spectra in Fig. 6 show that band gap of Gfs is about 2.80 eV. The nanggrass may enhance the optical performance of TiNTs due to its increased surface area and potential for light trapping³¹. Additionally, we propose that this behavior results from flaws that create extra states at the band gap close to the valence band (VB) or the conduction band (CB). Oxygen vacancies and titanium interstitials are examples of material imperfections that can change a material's electrical and optical characteristics³². By offering a direct channel for electron transport, the vertically oriented nanotubes minimize bulk defects and lower charge recombination rates. A greater percentage of photo-generated electrons and holes are available for the photocatalytic processes affecting the degradation process. Better photon harvesting is possible by the enhanced light scattering that nanotubular structures may provide within their inner channels. This may also promote the creation of

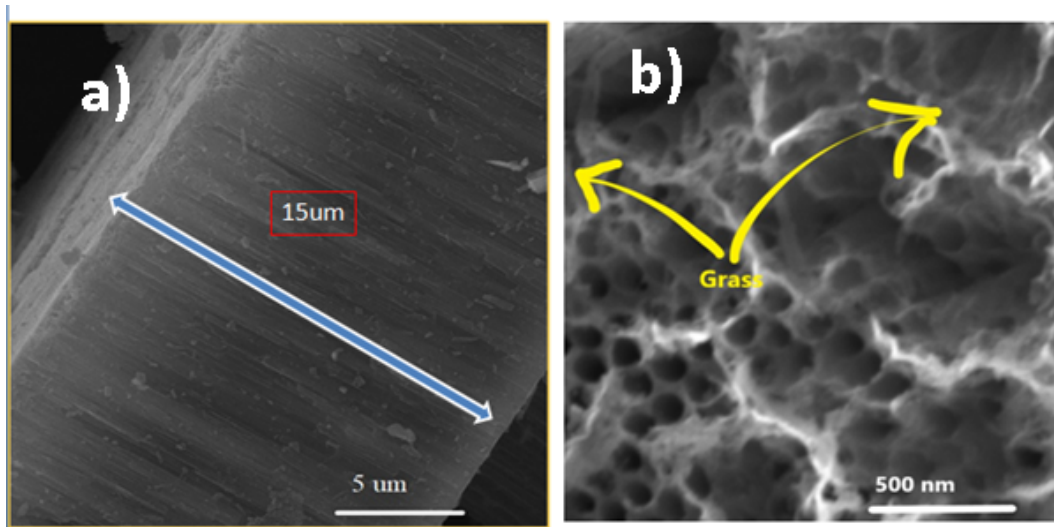


FIG. 3: FE-SEM images for the prepared Gfs-TiNTs (a,b).

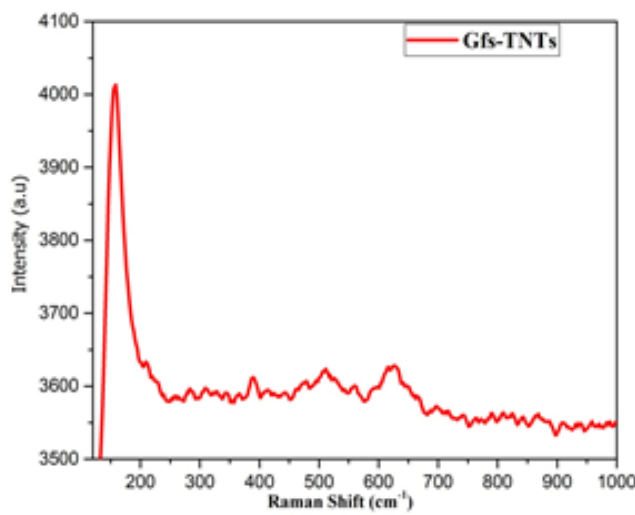


FIG. 4: Raman spectroscopy for the prepared Gfs-TiNTs.

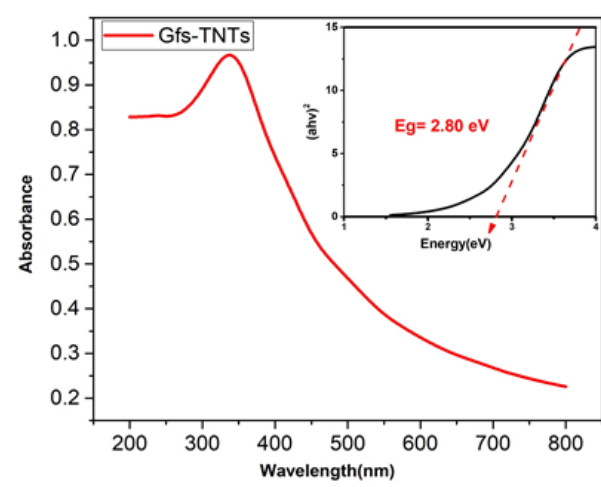


FIG. 5: UV-visible Absorbance spectra and Bandgap estimation for Gfs-TiNTs.

electron-hole pairs, essential for photocatalysis, by increasing the use of the UV-visible light spectrum^{33,34}.

D. Photocatalytic Degradation Performance

Photocatalytic EBT dye degradation is determined by UV-visible spectroscopy using Grass free amorphous

Titania nanotubes photo-catalyst. Photocatalytic test is carried out under Xenon lamp for 80 min . The standard calibration curve assesses the rate of sample degradation at its peak. Beer-Lambert’s law states that the concentration of a dye is proportional to its absorbance. Degradation (%) is computed using the formula below.

TABLE II: Previous Studies for the Photodegradation of various Dyes.

Samples	Dye	Time	Source / Degradation	Ref.
TiO ₂ -based photocatalyst	EBT	3 hours	UV light / 80%	41
Ni:TiO ₂ nanocomposites	EBT	180 min	Visible lamp / 90%	42
Anodized TiO ₂ nanotubes	Methylene blue	180 min	UV light / 35%	33
Free-standing TiO ₂ TiNts	Methylene blue	150 min	UV light / 38%	36
TiO ₂ NPs	EBT	150 min	UV light / 25%	35
Vertically aligned TiNts	Methylene blue	180 min	UV light / 30%	34
Gfs.-TiNts	EBT	80 min	Xenon lamp / 40%	Present Work

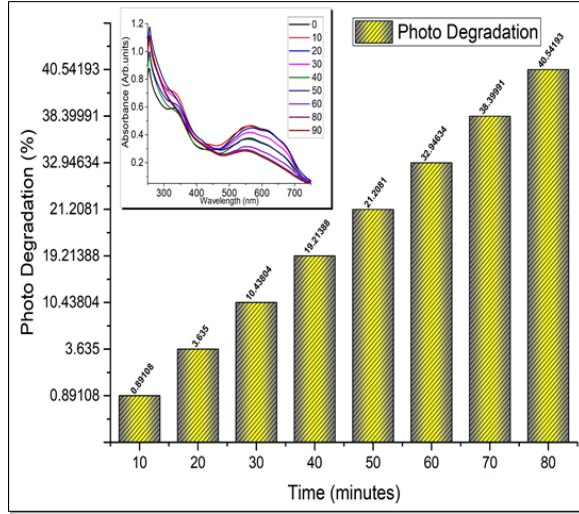


FIG. 6: The photodegradation of EBT dye using Gfs-TiNts.

$$\% \text{ Degradation} = [(C_o - C_T) / C_o] \times 100$$

C₀ and C_T represent the highest and lowest concentrations of EBT dye before and after photo irradiation respectively. Fig. 5 depicts the rate of photo degradation. The photo catalytic EBT dye with Gfs-nanotubes shows 40% degradation in only 80 min. When exposed to Ux light, the degradation process is started by the photo generated electron-hole pairs in the nanotubes. The electrons of the valence band (VB) will move to the conduction band (CB). Then the holes and electrons photo-generated will be transported to the TiO₂/EBT dye solution interface and react with the adsorbed molecules. After that, the dye molecules are oxidized when holes (h⁺) combine with adsorbed water or hydroxide ions to generate ·OH radicals. The O₂*⁻ is

created and this subsequent reaction breaks down the dye. The specific surface area is greatly increased by the nanotubular structure and further by the grassy architecture. This increased surface area can increase the interaction between the dye and photo superoxide anions (O₂*⁻) and hydroxyl radicals (·OH) by providing a large number of active sites for the adsorption of EBT dye molecules. The production of reactive oxygen species (superoxide anions and hydroxyl radicals) may be enhanced by the high aspect ratio of the TiNts, which also guarantee the effective photon absorption in the UV range³⁴⁻³⁶.

Thus, this study found that manufactured nanotubes can oxidize EBT dye by producing electron-hole pairs when exposed to light. The rate of photo degradation is determined by the electrostatic interaction between dye molecules and the catalyst surface. The surface of nanotubes is grassy and less porous that resulted in less degradation rate. Another element that may increase photocatalytic activity is nanoporosity of TiNts, which creates additional trapping sites on the catalyst surface because of its larger specific surface area^{32,37,38}. By trapping photo generated electrons and lowering the conduction band, these locations slow down the rate of recombination. By improving material transfer, nanoporous shapes enable more molecules to adsorb onto the material's surface^{38,39}. The comparison from literature for the photodegradation of EBT dye by utilizing TiNts is presented in Table II. In our case, the grassy materials' tubular shape may also offer a high surface-to-volume ratio, increasing the quantity of active sites accessible for photocatalytic processes. This structural characteristic directly affects photocatalytic performance by facilitating the effective adsorption of EBT dye molecules on the surface.

V. CONCLUSION

In current study, grassy free standing TiO₂ nanotubes were successfully synthesized by 2 -step anodization

method and assessed for their photocatalytic efficiency in EBT dye degradation. The FESEM analysis revealed the grassy nanotubular architecture with length and outer diameter around $15\mu\text{m}$ and $60-100\text{nm}$, respectively. The distinctive grassy morphology of the nanotubes improved the surface area and light-harvesting capabilities, contributing to noteworthy photocatalytic performance. The Raman analysis has revealed the presence of anatase phase as a result of mild crystallization occurred during water dipping treatment. From UV-visible characterization the band gap of Gfs-TiNTs estimated around 2.80eV . The grassy aligned tubular morphology, presence of anatase phase, reduced bandgap and light absorption towards longer wavelengths has greatly affected the surface area assisted photon absorption, and light trapping behavior in TiNTs. Under optimized anodization conditions the Gfs-TiNTs achieved 40% degradation of the EBT azo dye in 80 minutes under UV light exposure. This study also highlighted the importance of tailored nanotubular grassy structures in refining photocatalytic organic dyes degradation and flagging for further improvements in wastewater treatment technologies.

DECLARATION OF COMPETING INTEREST

The authors have no conflicts to disclose.

ACKNOWLEDGMENTS

We are pleased to acknowledge “1st International Conference on Sciences for Future Trends (ICSFT)- University of Lahore, Sargodha campus”, for providing a valuable platform for sharing this research.

REFERENCES

- ¹N. M. Mahmoodi and M. Arami, “Degradation and toxicity reduction of textile wastewater using immobilized titania nanophotocatalysis,” *Journal of Photochemistry and Photobiology B: Biology* **94**, 20–24 (2009).
- ²N. Jabeen, A. Hussain, F. Shahid, and M. M. Hessian, “Enhanced performance of $\text{Na}_4\text{Ti}_5\text{O}_{12}$ nanowall arrays for next-generation pseudocapacitors through sodiation treatment,” *FlatChem* **47**, 100715 (2024).
- ³X. Cheng *et al.*, “Preparation and characterization of palladium nano-crystallite decorated TiO_2 nano-tubes photoelectrode and its enhanced photocatalytic efficiency for degradation of diclofenac,” *Journal of Hazardous Materials* **254**, 141–148 (2013).
- ⁴I. Khan *et al.*, “Heterogeneous photodegradation of industrial dyes: An insight to different mechanisms and rate affecting parameters,” *Journal of Environmental Chemical Engineering* **8**, 104364 (2020).
- ⁵M. S. Oliveira *et al.*, “Polymyxin b and colistimethate are comparable as to efficacy and renal toxicity,” *Diagnostic Microbiology and Infectious Disease* **65**, 431–434 (2009).
- ⁶H. Sopha *et al.*, “Recent advances in TiO_2 nanotube layers—a mini review of the latest developments in nanotube preparation and applications in photocatalysis and microwave sensing,” *Nano Select* **5**, 2300140 (2024).
- ⁷L. Niu *et al.*, “Difference in performance and mechanism for methylene blue when TiO_2 nanoparticles are converted to nanotubes,” *Journal of Cleaner Production* **297**, 126498 (2021).
- ⁸R. Narayanan *et al.*, “Anodic TiO_2 nanotubes from stirred baths: hydroxyapatite growth & osteoblast responses,” *Materials Chemistry and Physics* **125**, 510–517 (2011).
- ⁹Z. B. Xie and D. J. Blackwood, “Effects of anodization parameters on the formation of titania nanotubes in ethylene glycol,” *Electrochimica Acta* **56**, 905–912 (2010).
- ¹⁰M. Balakrishnan and R. Narayanan, “Synthesis of anodic titania nanotubes in $\text{Na}_2\text{SO}_4/\text{NaF}$ electrolyte: A comparison between anodization time and specimens with biomaterial based approaches,” *Thin Solid Films* **540**, 23–30 (2013).
- ¹¹D. Regonini *et al.*, “Factors influencing surface morphology of anodized TiO_2 nanotubes,” *Electrochimica Acta* **74**, 244–253 (2012).
- ¹²A. Talla *et al.*, “Effect of annealing temperature and atmosphere on the structural, morphological and luminescent properties of TiO_2 nanotubes,” *Physica B: Condensed Matter* **640**, 414026 (2022).
- ¹³T. Ghani *et al.*, “Photovoltaic performance of TiO_2 nanotubes anodized under different voltages,” *Materials Proceedings* **17**, 24 (2024).
- ¹⁴R. K. Shah, “Facile synthesis of novel nis-analcime composite for the efficient photocatalytic degradation of eriochrome black t dye,” *International Journal of Environmental Analytical Chemistry* **102**, 8331–8345 (2022).
- ¹⁵N. Khan *et al.*, “Adsorption of $\text{Cu}(\text{II})$ ion through functionalized nylon 66 and their utilization as photocatalyst for the photodegradation of eriochrome black t dye in aqueous medium,” *Fibers and Polymers* **23**, 1266–1274 (2022).
- ¹⁶H. Al-Zoubi *et al.*, “Comparative adsorption of anionic dyes (eriochrome black t and congo red) onto jojoba residues: isotherm, kinetics and thermodynamic studies,” *Arabian Journal for Science and Engineering* **45**, 7275–7287 (2020).
- ¹⁷S. Taghavi Fardood *et al.*, “Green synthesis, characterization, and photocatalytic activity of cobalt chromite spinel nanoparticles,” *Materials Research Express* **7**, 015086 (2020).
- ¹⁸P. Franco *et al.*, “Photocatalytic degradation of eriochrome black-t azo dye using eu-doped ZnO prepared by supercritical antisolvent precipitation route: A preliminary investigation,” *Topics in Catalysis* **63**, 1193–1205 (2020).
- ¹⁹B. Pal, R. Kaur, and I. S. Grover, “Superior adsorption and photodegradation of eriochrome black-t dye by Fe^{3+} and Pt^{4+} impregnated TiO_2 nanostructures of different shapes,” *Journal of Industrial and Engineering Chemistry* **33**, 178–184 (2016).
- ²⁰E. Montakhab, F. Rashchi, and S. Shebani, “Modification and photocatalytic activity of open channel TiO_2 nanotubes array synthesized by anodization process,” *Applied Surface Science* **534**, 147581 (2020).
- ²¹M. A. A. Taib *et al.*, “Formation of grassy TiO_2 nanotube thin film by anodisation in peroxide electrolyte for $\text{Cr}(\text{VI})$ removal under ultraviolet radiation,” *Nanotechnology* **31**, 435605 (2020).
- ²²R. Ashvega Sherly *et al.*, “ H_2O_2 -assisted photo-electrocatalytic and photocatalytic degradation of methyl violet by Cu-modified TiO_2 nanotube arrays,” *Optical Materials* **155**, 115870 (2024).

- ²³O. Zakir *et al.*, “A review on tio2 nanotubes: synthesis strategies, modifications, and applications,” *Journal of Solid State Electrochemistry* **27**, 2289–2307 (2023).
- ²⁴D. Kim, A. Ghicov, and P. Schmuki, “Tio2 nanotube arrays: Elimination of disordered top layers (“nanograss”) for improved photoconversion efficiency in dye-sensitized solar cells,” *Electrochemistry Communications* **10**, 1835–1838 (2008).
- ²⁵S. Dasarathan *et al.*, “Free-standing tio2 nanograssy tubular hybrid membrane for polysulfide trapping in li-s battery,” *RSC Advances* **13**, 8299–8306 (2023).
- ²⁶T. Ohsaka, F. Izumi, and Y. Fujiki, “Raman spectrum of anatase, tio2,” *Journal of Raman Spectroscopy* **7**, 321–324 (1978).
- ²⁷P. Ramasamy *et al.*, “A general approach for synthesis of functional metal oxide nanotubes and their application in dye-sensitized solar cells,” *RSC Advances* **4**, 2858–2864 (2014).
- ²⁸M. Salari, K. Konstantinov, and H. K. Liu, “Enhancement of the capacitance in tio2 nanotubes through controlled introduction of oxygen vacancies,” *Journal of Materials Chemistry* **21**, 5128–5133 (2011).
- ²⁹A. Lamberti *et al.*, “Ultrafast room-temperature crystallization of tio2 nanotubes exploiting water-vapor treatment,” *Scientific Reports* **5**, 7808 (2015).
- ³⁰U. Diebold, “The surface science of titanium dioxide,” *Surface Science Reports* **48**, 53–229 (2003).
- ³¹S. Ahmad *et al.*, “Excellent photocatalytic and antibacterial performance of silver and cobalt doped mno nanoparticles,” *Physica Scripta* **98**, 115023 (2023).
- ³²H. Fraoucene *et al.*, “Tio nanotubes with nanograss structure: The effect of the anodizing voltage on the formation mechanism and structure properties,” *Journal of Electronic Materials* **48**, 2046–2054 (2019).
- ³³P. Roy, S. Berger, and P. Schmuki, “Tio2 nanotubes: synthesis and applications,” *Angewandte Chemie International Edition* **50**, 2904–2939 (2011).
- ³⁴S. P. Albu *et al.*, “Self-organized, free-standing tio2 nanotube membrane for flow-through photocatalytic applications,” *Nano Letters* **7**, 1286–1289 (2007).
- ³⁵X. Chen and S. S. Mao, “Titanium dioxide nanomaterials: synthesis, properties, modifications, and applications,” *Chemical Reviews* **107**, 2891–2959 (2007).
- ³⁶D. Zagoraios *et al.*, “Electrochemical promotion of methane oxidation over nanodispersed pd/co3o4 catalysts,” *Catalysis Today* **355**, 910–920 (2020).
- ³⁷H. Far *et al.*, “High-performance photocatalytic degradation of nio nanoparticles embedded on α -fe2o3 nanoporous layers under visible light irradiation,” *Journal of Materials Research and Technology* **19**, 1944–1960 (2022).
- ³⁸W. Xu *et al.*, “Nanoporous cus with excellent photocatalytic property,” *Scientific Reports* **5**, 18125 (2015).
- ³⁹S. Shaikh *et al.*, “Mechanistic insights into the antimicrobial actions of metallic nanoparticles and their implications for multidrug resistance,” *International Journal of Molecular Sciences* **20**, 2468 (2019).
- ⁴⁰J. Yan *et al.*, “Understanding the effect of surface/bulk defects on the photocatalytic activity of tio2: anatase versus rutile,” *Physical Chemistry Chemical Physics* **15**, 10978–10988 (2013).
- ⁴¹R. A. Putri *et al.*, “Synthesis of tio2-based photocatalyst from indonesia ilmenite ore for photodegradation of eriochrome black-t dye,” *Water, Air, & Soil Pollution* **234**, 554 (2023).
- ⁴²A. Kumar and G. Pandey, “Photocatalytic degradation of eriochrome black-t by the ni: Tio2 nanocomposites,” *Desalination and Water Treatment* **71**, 406–419 (2017).